analytical chemistry

Article

Cite This: *Anal. Chem.* 2018, 90, 10239−10248

pubs.acs.org/ac

Lipid Mediator Quantification in Isolated Human and Guinea Pig Airways: An Expanded Approach for Respiratory Research

Johan Kolmert,[†,‡,§] Alexander Fauland,[†,§] David Fuchs,[†] Jesper Säfholm,[‡] Cristina Gómez,[†] Mikael Adner,[‡] Sven-Erik Dahlén,[*,‡] and Craig E. Wheelock[*,†]

[†]Division of Physiological Chemistry II, Department of Medical Biochemistry and Biophysics, Karolinska Institutet, 17177 Stockholm, Sweden

[‡]Institute of Environmental Medicine, Experimental Asthma and Allergy Research Unit, Karolinska Institutet, 17177 Stockholm, Sweden

Supporting Information

ABSTRACT: The clinical importance of prostaglandins and leukotrienes in asthma is well recognized; however, the biochemical role of other lipid mediators (often termed oxylipins) in the regulation of airway tone and inflammation remains unclear. We therefore developed a workflow to investigate oxylipin physiology and pharmacology in two *in vitro* models, the intact human bronchus and the guinea pig trachea. Airways were isolated and smooth muscle contraction was measured in an organ bath following stimulation with either anti-IgE or ovalbumin. The associated release of oxylipins over time into the organ bath was quantified using three developed LC−MS/MS methods capable of collectively measuring 130 compounds. Oxylipin extraction recoveries were 71% on average, method accuracy was 90−98%, coefficient of variation was 4.3−9.4%, and matrix effects were on average 11%. At baseline, low levels of primarily prostaglandins and associated metabolites were observed in both tissue preparations. The mast cell-induced airway constriction caused release of leukotrienes and further elevations in prostaglandin levels. In total, 57 oxylipins from the human bronchus, and 42 from guinea pig trachea, were detected at 60 min post-stimulation in the organ bath. Chiral analysis demonstrated that 5-hydroxyeicosatetraenoic acid (5-HETE) in the human bronchus preparation was not produced by 5-LOX enzymatic activity (enantiomeric excess [ee] = 10%), as opposed to 12(*S*)-HETE, 14(*S*)-, and 17(*S*)-hydroxy docosahexaenoic acid (HDoHE; ee = 100%), highlighting that chiral chromatography is necessary for correct biological interpretation. Unexpectedly, prostaglandin D_2 and its metabolites remained elevated 24 h after the challenges, suggesting a sustained activation of mast cells not previously described. The reported translational methodology provides a new platform for comprehensive studies to elucidate the origin and functions of individual oxylipins in various airway responses.

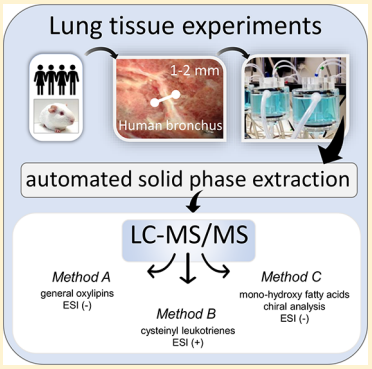

Prostaglandins (PG) and leukotrienes (LT) are established mediators of inflammation as evidenced by the therapeutic effects of nonsteroidal anti-inflammatory drugs (NSAIDs) and antileukotriene drugs, respectively.[1,2] They are synthesized in reactions where cellular activation liberates arachidonic acid (AA) from membrane stores for oxygenation by cyclooxygenases (COX) and the 5-lipoxygenase (5-LOX), respectively.[3] Related polyunsaturated fatty acids (PUFAs) may be metabolized via the same pathways as AA. There are also alternative enzymatic pathways for oxygenation of PUFAs, including lipoxygenases attacking other carbons in the AA backbone (e.g., 12-LOX and 15-LOX) and catalysis via cytochrome P450 (CYP450). Furthermore, nonenzymatic free radical-induced peroxidation (i.e., autoxidation) reactions generate multiple compounds (e.g., isoprostanes and mono-hydroxy fatty acids) from the same precursors.[4] To simplify discussions of the PUFA oxygenated metabolites, they are herein collectively referred to as oxylipins.[5]

Lipid products of the COX and LOX pathways are known to play fundamental roles in the pathophysiology of asthma.[6] For example, montelukast is a leukotriene receptor $CysLT_1$ antagonist that is used to treat asthma and allergy,[2] and the prostaglandin receptor CRTH2 is being investigated as a potential new therapeutic target.[7] In addition, the involvement of COX-derived oxylipins in disease pathology is well demonstrated by aspirin intolerant asthma (AIA), in which administration of aspirin can elicit severe disease exacerbations.[8] However, in most instances there is no comprehensive understanding of the relative functional importance of the broader range of compounds that may be formed from different PUFAs. It is often unclear how the flow of fatty acid substrates along alternate pathways is regulated physiologically, in different pathological states or by drug intervention. Available data are mostly limited to simplified cellular models[9] or to the measurement of a select panel of metabolites in tissues.[10] There is a need to progress the understanding of the

Received: April 13, 2018
Accepted: July 28, 2018
Published: July 28, 2018

DOI: 10.1021/acs.analchem.8b01651
Anal. Chem. 2018, 90, 10239−10248

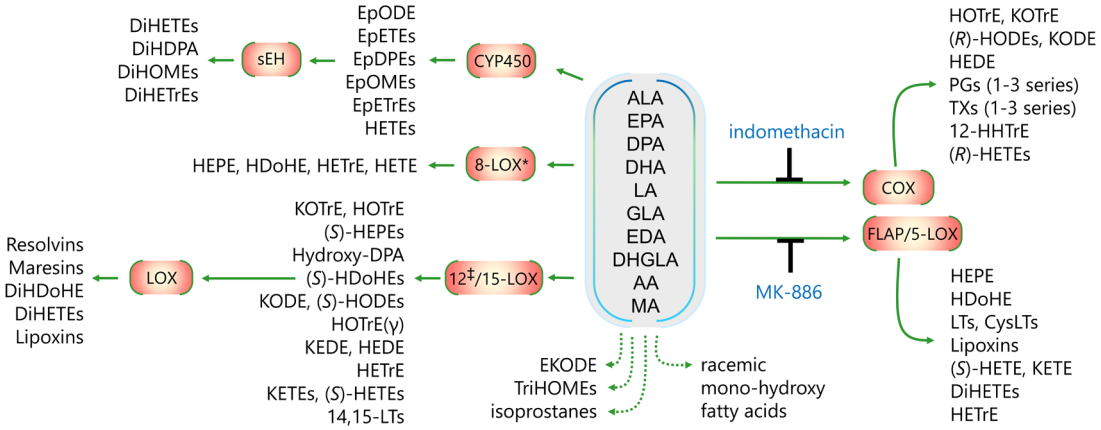

Figure 1. Oxylipin pathways quantified using Methods A−C. Indomethacin and MK-886 were used to inhibit cyclooxygenase (COX) and five lipoxygenase activating protein/5-lipoxygenase (FLAP/5-LOX), respectively. Nonenzymatic or unknown synthetic route is indicated by the green dotted line. Oxylipin stereochemistry is shown for those species included in Method C. The order of dual lipoxygenation (e.g., DiHDoHE, DiHETEs, Lipoxins) is interchangeable. Abbreviations: arachidonic acid (AA), α- and γ-linolenic acids (ALA, GLA), dihomo-gamma-linolenic acid (DHGLA), docosahexaenoic acid (DHA), docosapentaenoic acid (DPA), eicosapentaenoic acid (EPA), linoleic acid (LA), 5,8,11-eicosatrienoic acid (mead acid; MA), 11,14- eicosadienoic acid (EDA), soluble epoxide hydrolase (sEH), and cytochrome P450 (CYP450). Lipid nomenclature is provided in Table S-1. *8-LOX has not been described in humans. ‡The enzyme 12R-LOX can produce 12(*R*)-HETE.[24]

relationship between biosynthesis and biological functions in intact tissues by measuring a broader panel of compounds.

This article reports a workflow to enable in-depth analysis of oxylipin biology in the airways. We describe how the media surrounding isolated intact human and guinea pig airway segments is sampled for oxylipin quantification concomitantly with the assessment of the functional response, including the effects of drug interventions. The LC−MS/MS approach presented herein, in combination with automated extraction, renders it possible to simultaneously monitor airway responses and release of 130 oxylipins representing the major synthetic pathways (Figure 1). One important aspect of the workflow to highlight is the inclusion of a chiral separation step for the monohydroxy fatty acids. This approach renders it possible to determine the synthetic source of the compound.[11] Enzymatically catalyzed reactions result in the biosynthesis of a single enantiomer, whereas autoxidation produces a racemic mixture.

A strength of the workflow is the use of the classical pharmacologic organ bath bioassay methodology for the parallel recording of functional responses in the isolated tissue preparation. The use of intact tissue explants is a particular advantage of this experimental system because it preserves cellular organization and differentiation as well as natural signaling cascades that may disappear in cell models or constructed cell-lines. In addition, the conducted experiments are performed under noninflamed conditions. Together, these parameters enable investigation of the kinetics of basal physiological and biochemical effects simultaneously, which is not possible in the clinical setting. Major findings have earlier been accomplished by using this methodology, for example, the discovery of PGs, LTs, endothelin, and nitric oxide.[12,13] To validate this strategy, we employed a model in which the airways were exposed to either anti-IgE or allergens to induce a mast cell-release of bronchoconstrictive mediators. We demonstrated how this activation mechanism triggers contractions and specific patterns of oxylipin release in freshly isolated human small bronchi and intact guinea pig airways over time. Results were in agreement with our earlier findings reporting potent effects by the release of PGs and LTs.[14,15] However, unexpectedly, prostaglandin D_2 and its metabolites remained elevated 24-h after the challenges, suggesting a sustained activation of mast cells not previously described.

We propose that this combined research methodology offers a new discovery platform with the potential to provide insight into biochemical mechanisms related to inflammatory cascades in the airways and the identification of novel drug targets. It should be appreciated that the methodology may be applied in multiple research areas, including blood vessels, gastrointestinal segments, and urogenital organs, which can be studied in a similar approach.

MATERIALS AND METHODS

Chemicals and Reagents. All oxylipin standards were purchased from Cayman Chemical (Ann Arbor, MI), with the exception of 12,13-EpODE, 9,10,13-TriHOME, and 9,12,13-TriHOME, which were obtained from Larodan (Solna, Sweden). Lipid mediator nomenclature for all compounds is provided in Table S-1. An LC−MS/MS system suitability test (SST) mix was prepared in 84% organic solvent with the 109 oxylipins included in Method A to assess overall instrument sensitivity and performance. The final concentrations of oxylipin standards in the SST mix were 0.5−100 ng/mL.

Human Tissue Preparation. Macroscopically healthy human lung tissue was obtained by consent from 4 females and 3 male patients, median age 65 years (59−77), undergoing surgical lobectomy at the Karolinska University Hospital. Within 3 h of the resection, microscopy-aided dissection of up to 16 isolated bronchial rings with inner diameters of ≤2 mm was performed. The small airway segments were placed in culture plate wells containing Dulbecco's modified Eagle medium (DMEM; Gibco, Auckland, NZ) supplemented with 1% penicillin (100 IU/mL; Sigma-Aldrich (St. Louis, MO)) and streptomycin (100 μg/mL; Gibco) under sterile conditions and kept overnight in a humidified incubator (37 °C at 95% O_2 and 5% CO_2) before functional experiments were performed the next day. Human tissue use was approved by the Stockholm south regional ethical review board (ref. no. 2010/181-31/2).

Guinea Pig Sensitization Procedure and Tissue Preparation. Male albino guinea pigs (Dunkin-Hartley;

DOI: 10.1021/acs.analchem.8b01651
Anal. Chem. 2018, 90, 10239−10248

400−450 g; n = 3) were sensitized by a single intraperitoneal injection, containing 100 μg grade V: chicken egg albumin (OVA) and 0.1 g aluminum hydroxide dissolved in 0.8 mL of sterile phosphate buffer saline (PBS), 28 days prior to organ bath experiments. Given that guinea pigs do not synthesize vitamin C, chow was supplemented with 1500 mg/kg vitamin C. Animals were sacrificed by inhalation of CO_2 followed by rapid removal of the heart-lung-package that was placed in ice-cold Krebs-Ringer PSS buffer (Krebs buffer). The guinea pig trachea was gently dissected from the surrounding connective tissue, cut into eight intact rings of equal length, containing between two and three cartilage rings of 2−5 mm thickness. Animals used in this study were approved by the Swedish animal experimentation ethical review board (ref no. N143/14).

Time Dependent Bronchoconstriction Assay. For human isolated bronchi, the rings were mounted in a 5 mL myograph (Organ Bath model 700MO, DMT A/S, Aarhus, Denmark) and for guinea pig experiments, tracheal rings were mounted in 5 mL organ baths (EMKA, France). The amount of tissue in each well ranged from 1.5 to 4.0 mg. Isometric changes of smooth muscle tension were recorded (ADInstruments Ltd., Hastings, U.K) and displayed using LabChart 7.0.3 (ADInstruments) as Newtonian force (E). The tissues were submerged in Krebs buffer and kept at 37 °C, with constant bubbling of carbogen (5% CO_2 in O_2) to maintain pH 7.4 during the experiment. To study the antigen-induced response in the human bronchus, 5.2 μg/mL of anti-IgE, and in the guinea pig trachea, 0.1 mg/mL OVA, was added to obtain a maximal antigen induced smooth muscle contraction.[14,15] The contractile response was then investigated in the absence and presence of indomethacin (3 μmol/L), MK-886 (10 μmol/L) or their combined presence (for human tissue). In all experiments using tissue, several segments from each donor were dissected so that each pharmacological treatment had its own negative PBS control (i.e., parallel segments). Segments from the same three patients were used in the experiments for Figures 2A and 3−5. Three additional patient samples were used for the kinetic release experiments in Figure 2C−E, and one individual was used for sample freeze−thaw evaluation.

Oxylipin LC−MS/MS Methods. Standard curves and internal standard solutions were prepared for three different analytical methods: Method A, eicosanoids and related compounds (i.e., oxylipins) measured in negative ionization mode; Method B, cysteinyl leukotrienes (CysLTs) measured in positive ionization mode; and Method C, chiral analysis of selected monohydroxy fatty acid compounds measured in negative ionization mode (Table S-1). For Method A (109 analytes), Method B (3 analytes), and Method C (18 analytes), stock solutions were diluted in methanol to a final concentration of 2 μg/mL. From these stock solutions, a combined calibration curve solution for Methods A and B was diluted to obtain an 11-point calibration curve (range, 0.002−834 ng/mL). MRM noise level and electrospray response influences the final linear dynamic range, which consequently varied between oxylipins. Therefore, the injected 11-point calibration curve ensured that a minimum of 6 calibration levels were available for calculating the concentration of each oxylipin using the LLOQ criteria stated below and with linearity R^2 > 0.98. For Method C, 18 chiral oxylipin standards were pooled into a single stock solution with an individual analyte concentration of 1.2 μg/mL and a final diluted calibration curve range of 0.17−342.9 ng/mL having a minimum of 6 calibration curve points. The internal standards (IS) consisted of a combined mix of 42 deuterated oxylipins for which the concentration of individual analytes was adjusted so that the average electrospray ionization (ESI) response was ∼10% of the highest calibration curve point. Prior to sample extraction, the IS mix containing the 42 deuterated standards was added to each sample in order to correct for any variations arising from the various sample preparation steps and variations in the electrospray ionization. On the day of analysis, 10 μL of the IS working solution and 10 μL of Milli-Q water were added to 50 μL of each calibration level aliquot resulting in a final solvent composition of methanol/water (6:1, v/v). The lower limit of quantification (LLOQ) was defined as the lowest calibration level having a signal-to-noise ratio (S/N) >5 and a measured concentration ≤20% of the nominal. Before data acquisition, a system suitability test was performed to ascertain instrument performance. Analyses were performed using an UPLC Acquity coupled to a Xevo TQ-S mass spectrometer system (Waters, Milford, MA). Details on instrument operating parameters and the properties of Methods A−C are summarized in Table S-2, with a brief overview provided below.

Method A: Oxylipins. A BEH C_{18} column (2.1 mm × 150 mm, 1.7 μm, Waters, Milford, MA) was used with mobile phase solvents A (water with 0.1% of acetic acid) and B (acetonitrile/isopropanol 90:10, v/v) at a flow rate of 0.5 mL/min. Gradient elution was performed with 80% of A as the starting condition, linearly decreased to 65% at 2.5 min, to 60% at 4.5 min, to 58% at 6 min, to 50% at 8 min, to 35% at 14 min, to 27.5% at 15.5 min, and to 0% at 16.6 min. The column was then washed with solvent B for 0.9 min and equilibrated to initial conditions. Method B: CysLTs. The same column as in Method A was used, but with mobile phase solvents A (water with 0.2% of formic acid) and B (acetonitrile/isopropanol 90:10, v/v + 0.2% formic acid) at a flow rate of 0.45 mL/min. Gradient elution was initiated with 60% of A, linearly decreased to 50% at 4.25 min and to 5% at 4.5 min. The column was then washed with 95% of solvent B for 3 min and equilibrated to initial conditions. Method C: chiral separation of monohydroxy fatty acids. A Chiral-Pak AD-RH analytical column (2.1 mm × 150 mm, 5 μm, Daicel Cooperation, France) was used with the same mobile phase composition as Method A at a flow rate of 0.6 mL/min. Gradient elution was performed with 40% of A, decreased linearly to 2% at 6.3 min, and to 0% at 6.4 min. The column was then washed with solvent B for 1 min and equilibrated to initial conditions for another 1 min. Methods A−C were characterized by means of defining the LLOQ, dynamic range and linear fit of the standard curve, accuracy and precision, as well as matrix effects and solid phase extraction (SPE) recoveries.

Oxylipin Extraction from Organ Bath Buffer. Each study sample was extracted once and used for Methods A−C as described below. Krebs buffer samples were withdrawn from the organ bath and processed immediately to avoid freeze/thaw cycles. For kinetic assessment, 0.5 mL was extracted and for pharmacological treatment, 3.5 mL was used. Each sample was spiked with 10 μL of the IS working solution and diluted (1:1) with extraction buffer (citric acid/Na_2HPO_4, pH = 5.6) prior to SPE. An automated liquid handling system, Extrahera (Biotage, Uppsala, Sweden), was equipped with 3 mL (3 cc/60 mg) Evolute Express ABN cartridges (Biotage, Uppsala, Sweden) conditioned and equilibrated with 2.5 mL of methanol and water, respectively. Loaded samples were

DOI: 10.1021/acs.analchem.8b01651
Anal. Chem. 2018, 90, 10239−10248

washed with 2 mL of water/methanol (90:10, v/v) and eluted with 2.5 mL of methanol. A volume of 30 μL glycerol/methanol (30:70, v/v) was added as trap solvent prior to evaporation using N_2 gas (TurboVap LV, Biotage, Uppsala, Sweden). Oxylipin extracts were reconstituted to a final volume of 70 μL in methanol/water (6:1, v/v) and filtered through a 0.1 μm polyvinylidenfluorid membrane spin filter (Amicron, Merck Millipore Cooperation, Billerica, MA) by 5 min centrifugation at 5 °C using 12 000 rcf. The positive pressure settings used for the Extrahera system are provided in the Supporting Information.

Stability of Oxylipins in the Organ Bath and during Freeze−Thaw. Oxylipin stability in the organ bath setting was evaluated as follows: the highest calibration curve solution (i.e., level 11) was spiked into 16 organ bath wells containing 5 mL of Krebs buffer and held at 37 °C for 0, 20, 40, and 60 min. A total volume of 3.5 mL was collected at each time point in replicates (n = 4) and processed according to Methods A and B. In a separate experiment using eight segments from one patient, 3.5 mL was withdrawn from the organ bath at the end of a human bronchi stimulation by anti-IgE or PBS (n = 4) and split into two aliquots for assessment of potential freeze−thaw effects. One aliquot was immediately snap-frozen in liquid N_2 and the other subjected to direct sample processing according to the described SPE method.

Quantification of Oxylipins from Tissue Incubations. After 60 min IgE stimulation, individual bronchi segments were washed 3 times with Krebs buffer and transferred to a 24-well plate with 1.5 mL of cell culture DMEM media and incubated at 37 °C for 24 h. Thereafter, 750 μL of tissue supernatant was extracted according to the above SPE protocol, and oxylipins were quantified.

Data Analysis and Statistics. For the organ bath experiments, the bronchoconstrictive Newtonian response was expressed in percentage of maximal contraction. In all figures reporting oxylipin concentrations, a correction-factor was applied incorporating the total extracted organ bath volume and the wet weight of the segment. Data are presented as average + SEM. For LC−MS/MS data, the TargetLynx application manager (Waters, Milford, MA) was used for calculating analyte concentrations from the corresponding calibration curve. Relative responses (peak area of analyte/peak area of IS) were used for analyte quantification. Table S-2 provides the matched IS for each oxylipin. Subsequent statistical analysis was performed using Students t-test. Statistical analysis was performed in GraphPad Prism v5.02 and v6.07 (GraphPad Software) and graphs were prepared in the same software, Excel 2016 (Microsoft Corp. USA) or TIBCO Spotfire nv.7.6.1. (USA).

RESULTS AND DISCUSSION

Characterization of the LC−MS/MS Methods. The initial efforts were centered on developing, optimizing and characterizing the three LC−MS/MS methods. Precautions were taken for all oxylipin standards to maintain analyte solubility and stability throughout the workflow. The calibration curve and stock solutions were therefore prepared in 100% methanol and stored under argon at −80 °C. The endogenous concentration range of individual oxylipins is wide and the corresponding ESI response varies on an oxylipin species-specific basis. Representative characteristics of Methods A−C averaged for all oxylipins demonstrated good linearity (R^2 = 0.996), LLOQ (0.016−0.7 ng/mL), accuracy, and precision (Tables S-2 and S-3). The inter- and intraday accuracies of Methods A−C were on average 95 ± 0.1% and 98 ± 0.1% at low concentration and 92.5% and 90.6% at high concentration, respectively (Table S-3). Precision measurements revealed coefficients of variation between 4.3 and 9.4% at both the low and high concentration levels.

The SPE recovery was evaluated using Krebs buffer solutions spiked with standards (1:20 diluted calibration level 11; concentration range 15−750 ng/mL), demonstrating an average recovery of 71%, with 90 analytes having >50% recovery (Table S-3). The reconstitution of dried extracts was carefully assessed and a 2-fold improvement in analyte average recovery was achieved following some small optimizations. The addition of 30 μL of 30% glycerol (dissolved in methanol) to the eluates before evaporation increased average recovery by 13%. Rinsing the inner surface of the collection tube with reconstitution solvent (70 μL methanol/water, 6:1 v/v) and vortexing for a minimum of 10 s during reconstitution provided an additional 19% increase (data not shown). It was not possible to inject a sample with LC-matched initial solvent composition (i.e., 20% organic) without compromising the solubility of several hydrophobic analytes. Therefore, the organic composition of the redissolvation mix was evaluated stepwise by the addition of 10−30% of water to the methanol. A final composition of 16% water was found suitable and markedly improved the Gaussian peak shape for polar (early eluting) analytes without affecting hydrophobic analyte solubility (Figure S-1). The automated SPE processing of samples was achieved in 65 min by use of the positive pressure handling system compared to 105 min using manual processing (a 38% reduction in time).

The matrix effects for Methods A−C were evaluated by adding the deuterated IS either to 84% methanol or Krebs buffer and comparing their corresponding measured and calculated concentrations. The obtained signal from oxylipins spiked into Krebs buffer ranged from 55 to 105% relative to compounds spiked into sample solvent, with 90% of the analytes evidencing <20% suppression (Table S-4). No changes in matrix effects were observed comparing extracted DMEM media with that of extracted Krebs buffer (data not shown).

Characterization of the Organ Bath System for Oxylipin Analysis. The production and stability of oxylipins in the organ bath system were determined to optimize the experimental parameters. A constant introduction of oxygen and carbon dioxide gas is necessary to maintain tissue viability and pH. However, because PUFAs are easily oxidized, it is possible that the high oxygen levels contribute to the formation of oxidized lipid species. To determine the magnitude and rates of oxylipin degradation, we spiked 112 oxylipin standards (included in Methods A and B) into the organ bath containing only buffer (i.e., in the absence of tissue) at 37 °C with a constant supply of O_2/CO_2. Samples were withdrawn after 0, 20, 40, and 60 min. We observed that 55 out of 112 oxylipins decreased in concentration by <50% during 60 min, while 25 out of 112 oxylipins maintained their concentration at >90% relative to the 0 min time point (Figure S-2). The rate of oxidation varied on an oxylipin species-specific basis (Table S-5). This observation should be taken into consideration for experimental design because many factors may affect the observed oxylipin levels. For example: (1) the baseline concentration in control segments, (2) the rate of degradation, (3) the volume of organ bath solution withdrawn for SPE

DOI: 10.1021/acs.analchem.8b01651
Anal. Chem. 2018, 90, 10239−10248

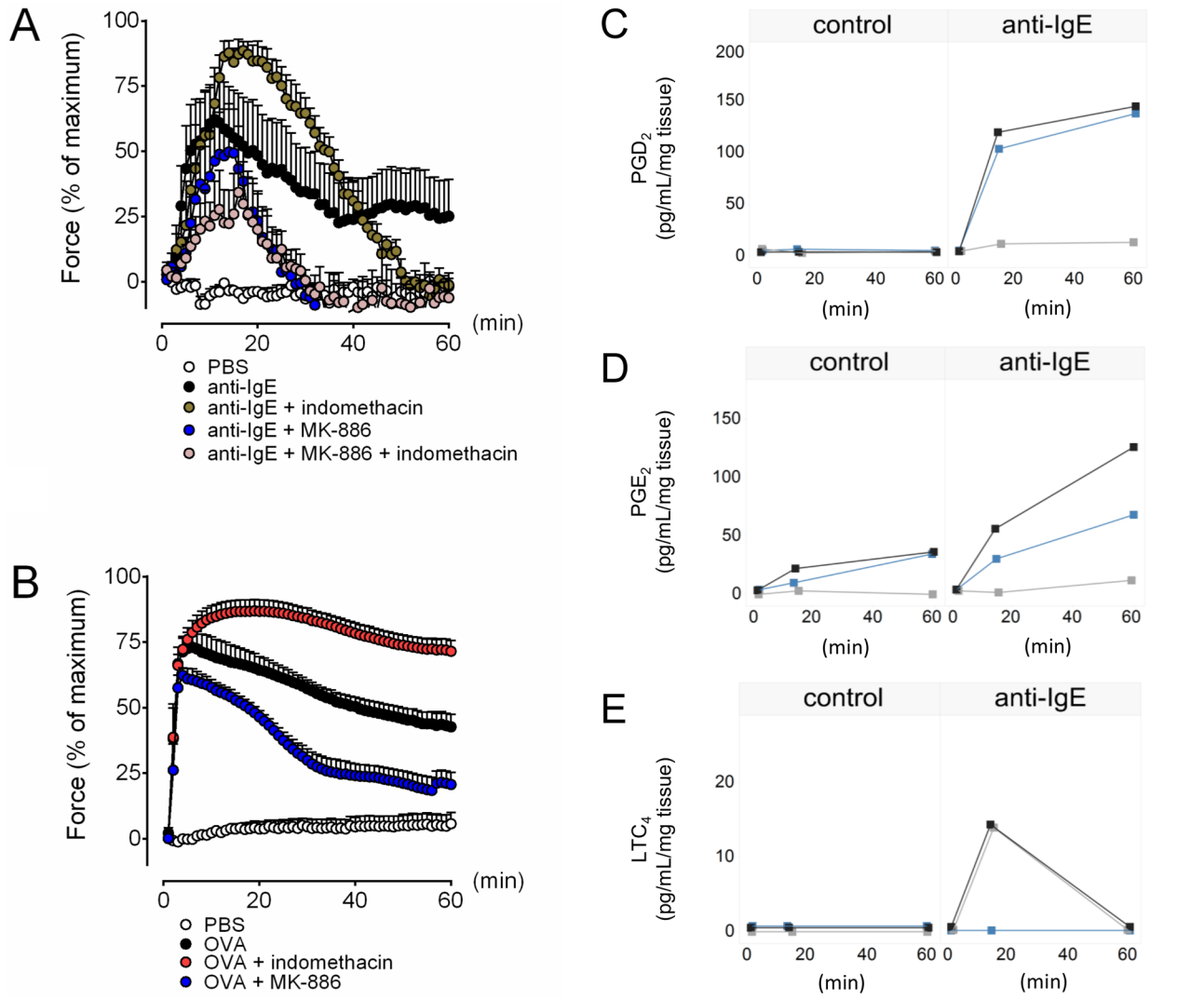

Figure 2. Stimulation of isolated human bronchus and guinea pig trachea. Stimulation of (A) isolated human bronchus with anti-IgE and (B) guinea pig trachea with OVA demonstrate a significant increase in contractile force after 15−20 min in both species (black dots). The force increased further by addition of nonselective cyclooxygenase inhibition (3 μM indomethacin, red dots) but decreased following addition of the FLAP/5-LOX inhibitor (10 μM MK-886, blue dots) or their dual combination in human bronchus demonstrated an even further decrease in contractile force (gray dots). (B) The same phenomenon was demonstrated in guinea pig trachea using OVA. Each treatment (colored dot) in panels A and B are represented by the average value calculated from 6 individual organ baths using 2 segments from each of 3 individuals. In total, 30 segments were utilized in panel A and 24 segments in panel B. Values are represented by average + standard error of the mean (SEM). Data from the same segments are shown in Figures 3, 4, and 5. In a separate experiment using three additional individuals (gray, blue, and black dots), panels C−E highlight the kinetic release of the two major COX products, PGD_2 and PGE_2, and the 5-LOX product LTC_4 into the organ bath Krebs buffer. Samples were withdrawn after 2, 15, and 60 min following anti-IgE stimulation. Each colored dot in panels C−E is the average of 2 segments. Phosphate buffer saline (PBS) served as negative control stimulant. Ovalbumin (OVA).

processing, and (4) the time between stimulation and buffer sample collection. The amount (mg) of tissue used, volume extracted, and selection of time-point are factors that can easily be adjusted in further experiments.

Based upon the reported loss of signal due to multiple freeze/thaw cycles,[16] we investigated the effect of freeze−thaw upon quantified oxylipin levels from extracted stimulated human tissue. We observed a loss of signal of 50−100% for 22 out of the 49 detected oxylipins (Table S-6). These observations indicate that freeze−thawing prior to SPE extraction can have a detrimental effect on the recovery of certain analytes. For example, PGD_2 was minimally affected (−12%) by freeze/thawing, while a 90% reduction in recovered signal was observed for 9-HOTrE (Figure S-3). Taking into consideration that oxylipins are relatively unstable compounds that are best preserved in organic solvent, all further experiments were performed by immediately applying SPE after sample collection from the organ bath.

The ability of the system to report functional responses in airway tissues was then assessed. Tissue segments were mounted in the organ baths and either anti-IgE or OVA was added to induce mast cell activation resulting in a persistent smooth muscle contraction in human bronchus preparation (E_{max} = 79 ± 10% vs control 7 ± 3%) and guinea pig trachea (E_{max} = 74 ± 6% vs control 9 ± 3%), respectively. The resulting contractile responses were continuously recorded following the stimulation. Anti-IgE binds the high affinity receptor FcεRI, abundantly located on the mast cell surface,

DOI: 10.1021/acs.analchem.8b01651
Anal. Chem. 2018, 90, 10239−10248

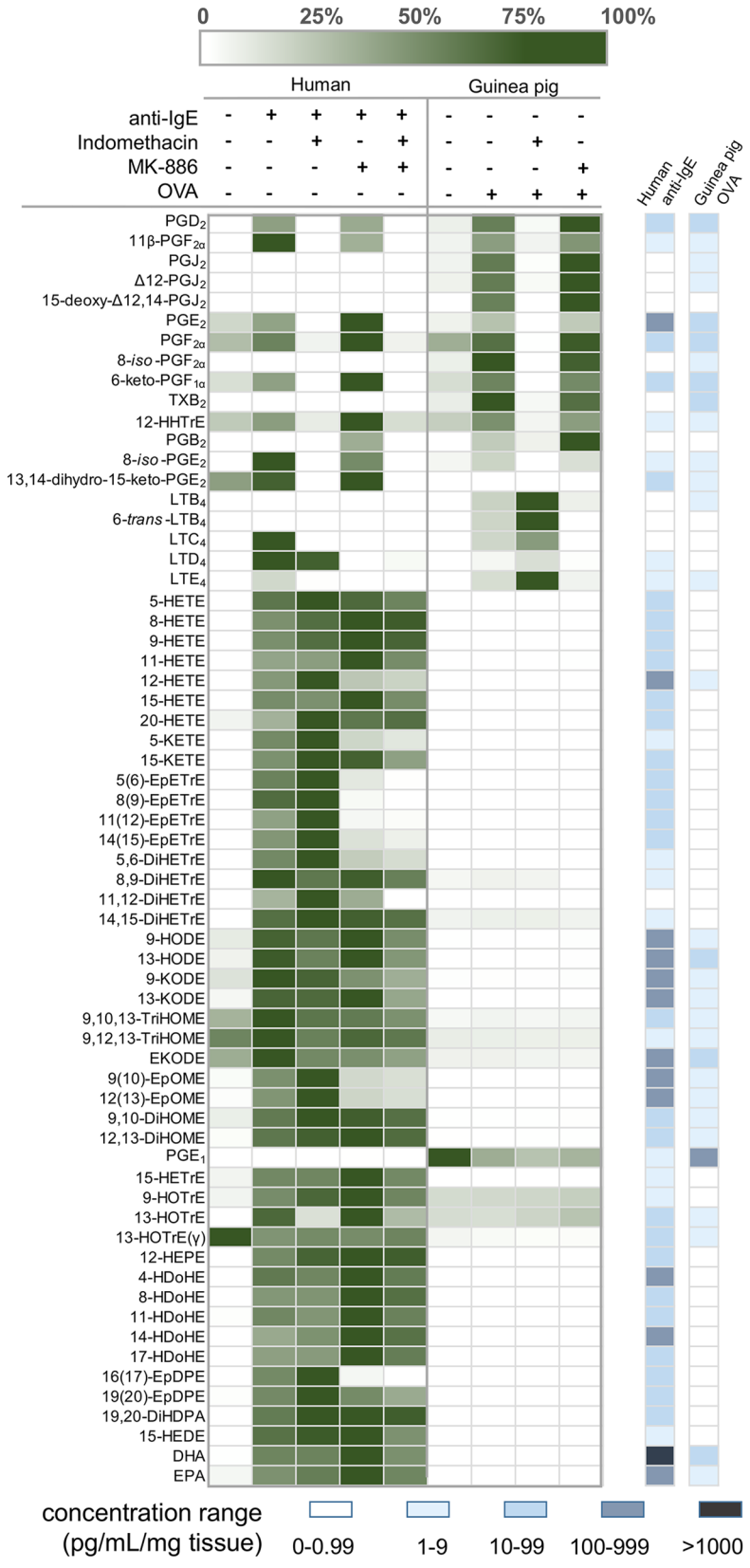

Figure 3. Alterations in oxylipin levels following anti-IgE or OVA stimulation in combination with COX or FLAP/5-LOX enzyme inhibition in human bronchus and guinea pig trachea. Each treatment condition was performed using duplicate segments from three individuals placed in separate organ bath wells ($n = 6$). For comparative purposes, the green heat map displays the concentration of each oxylipin normalized against the highest concentration (expressed as 100%) in each treatment across both species. For each oxylipin, dark green is 100% (highest concentration) and white is 0% (lowest concentration, below LLOQ). The blue heat map indicates five oxylipin concentration ranges wherein each compound is quantified following 60 min stimulation with anti-IgE in human bronchus and OVA in the guinea pig trachea. Phosphate buffer saline (PBS) served as a negative control. Ovalbumin (OVA).

DOI: 10.1021/acs.analchem.8b01651
Anal. Chem. 2018, 90, 10239−10248

causing calcium-mediated degranulation of mast cell mediators, which in turn stimulate a smooth muscle contraction (Figure 2A). Comparably, OVA triggers mast cell activation generating a similar contractile profile in guinea pig trachea (Figure 2B). Enzyme inhibitors were then added to preparations from both species to demonstrate their effect upon known oxylipin synthetic pathways. The nonselective NSAID indomethacin amplified contraction (E_{max} = 96 ± 4%, human and 87 ± 4%, guinea pig), reflecting the inhibition of prostanoid biosynthesis (Figure 2A,B, red trace).[15] We have previously demonstrated that PGE_2 has several actions that inhibit allergen-induced contractions, namely, to cause bronchorelaxation via the EP_4-receptors and to inhibit mast cell mediator release via EP_2 receptors.[14] In contrast, the 5-LOX activating protein (FLAP) inhibitor MK-886 demonstrated a reduced contractile response (E_{max} = 65 ± 16%, human and 63 ± 3%, guinea pig) presumably via inhibition of CysLT production (Figure 2A,B, blue trace).[17] CysLTs mediate powerful contractile response via the $CysLT_1$ receptor in humans and via the $CysLT_1$ and $CysLT_2$ receptor in the guinea pig.[18] A combined treatment with MK-886 and indomethacin (Figure 2A, gray trace) caused a 41% reduction in contractile force in the human bronchus preparation (E_{max} = 47 ± 15%). However, comparing area under the curve of anti-IgE response (black trace) vs the combined treatment (gray trace), it did not reach significance (Figure 2A).

The last step in the characterization was to assess the kinetic release of oxylipins into the organ bath by withdrawing samples at 2, 15, and 60 min following the stimulation of human bronchus preparation by anti-IgE. Two main COX products, PGD_2 and PGE_2, as well as the 5-LOX product LTC_4, reached detectable levels when maximum constriction was reached at 15 min (Figure 2C−E). The COX products continued to increase over the following 60 min compared to control (PBS). Accordingly, because the majority of oxylipins reached the highest concentration at 60 min, further experiments were only conducted using organ bath sampling at this time point.

Release of Oxylipins from *in Vitro* Stimulation of Human Bronchus and Guinea Pig Trachea. The developed workflow to detect oxylipin production was applied in both human bronchus and guinea pig trachea preparations. Both tissues were stimulated in the organ bath using the optimal conditions described above and the resulting oxylipin profiles after 60 min were acquired. In human bronchus, a total of 57 oxylipins were detected (S/N > 3) following stimulation with anti-IgE, of which 40 were increased in concentration relative to control ($p < 0.05$). In guinea pig trachea, a total of 42 oxylipins were detected (S/N > 3) following the stimulation by OVA, of which the levels of 11 prostanoids, LTB_4, isoprostanes, and all three CysLTs (LTC_4, LTD_4, and LTE_4) were significantly elevated (Figure 3, Tables S-7 and S-8).

The utility of the workflow to detect changes in oxylipin production was demonstrated by using pharmacological intervention to target the observed oxylipin biosynthesis. Indomethacin treatment was used to nonselectively inhibit both COX-1 and -2. The levels of 7 prostaglandins and the isoprostane 8-iso-PGE_2 were almost totally abolished by indomethacin in human bronchus ($p < 0.001$, Table S-7). Similarly, all prostanoids were decreased in guinea pig trachea, while the 5-LOX products LTB_4 and LTE_4 increased 3- to 4-fold ($p = 0.001$, Table S-8), a phenomenon not observed in the human tissue. Treatment with the FLAP/5-LOX inhibitor MK-886 in human tissue demonstrated a trend of decreased contraction force and was accompanied by a reduction in the CysLTs (Figure 3).

In addition, in the human bronchus experiments, several products of CYP activity, such as the arachidonic (EpETrEs) and linoleic acid epoxides (EpOMEs), were significantly decreased by ∼80% following FLAP/5-LOX inhibition (Figure 3). Compounds from these two classes have been reported to exert anti-inflammatory properties in human bronchus[19] and represent a potential therapeutic target for inflammatory lung disease.[20,21] Changes in EpETrEs and EpOMEs by inhibition of FLAP/5-LOX have not been reported previously and should be further investigated using the human bronchus preparation. These functional and biochemical observations are in agreement with current therapeutic intervention in which montelukast is used to antagonize the $CysLT_1$ receptor-mediated airway smooth muscle contraction.[2] In the guinea pig, a significant reduction in all leukotrienes, except for the short-lived LTD_4 (p = 0.203, Table S-8), was observed together with a reduction in the contractile force (E) (Figure 2B). In both species, MK-886 showed no effect on COX-derived oxylipins. DHA and EPA were abundant in guinea pig-derived samples, while their downstream metabolites were not.

From human bronchus, 9 DHA- and EPA-derived oxylipins were detected, of which 16(17)-EpDPE was markedly decreased by FLAP/5-LOX inhibition. The comprehensive oxylipin profiles acquired shared many similarities between the two species, although an additional 15 oxylipins were detected from human bronchus. The oxylipin release from human bronchus also displayed a more complex pattern with the additional detection of DHA, EPA, DHGLA, EDA, and LA downstream products. Despite the differences in absolute oxylipin levels between species, the same basic functional and biochemical responses were observed following stimulation as well as by COX and FLAP/5-LOX inhibition. Together these observations highlight the validity of using the guinea pig as a translational model for pharmacological interventions. In addition, guinea pigs can also be pretreated to induce chronic inflammation prior to organ bath stimulation.

Synthetic Origin of Observed Oxylipin Species. The chirality of lipid mediators has been shown to profoundly affect the observed biological activity[4,22] and provides important information on the synthetic route of the compound. The chirality of the monohydroxy fatty acids produced in human bronchus and guinea pig trachea following stimulation is generally not determined or measured in oxylipin profiling experiments. In total, we detected 13 chiral oxylipins in the organ bath. Of particular interest is the observation that equal amounts of 5(S)-HETE and 5(R)-HETE were produced from human bronchus preparation in all treatments (enantiomeric excess [ee] = 10), indicating that this compound was produced via autoxidation (Figure 4A and Figure S-4). In the absence of chiral chromatography, it would be likely concluded that the quantified levels of 5-HETE were indicative of 5-LOX activity. Conversely, the monohydroxy products of DHA evidenced enantioselectivity, producing 100% 14(S)-HDoHE (Figure 4B) and 17(S)-HDoHE as well as the arachidonic acid-derived 12(S)-HETE (ee = 100), identifying the 12/15-LOX enzyme as the synthetic source of these compounds. The ee was also calculated for detectable 11(S/R)-HETE, 15(S/R)-HETE, 9(S/R)-HODE, and 13(S/R)-HODE (Table 1), with the results evidencing substantial production from free-radical initiated peroxidation (ee = 0−41%). These findings demonstrate the importance of employing chiral chromatog-

DOI: 10.1021/acs.analchem.8b01651
Anal. Chem. 2018, 90, 10239−10248

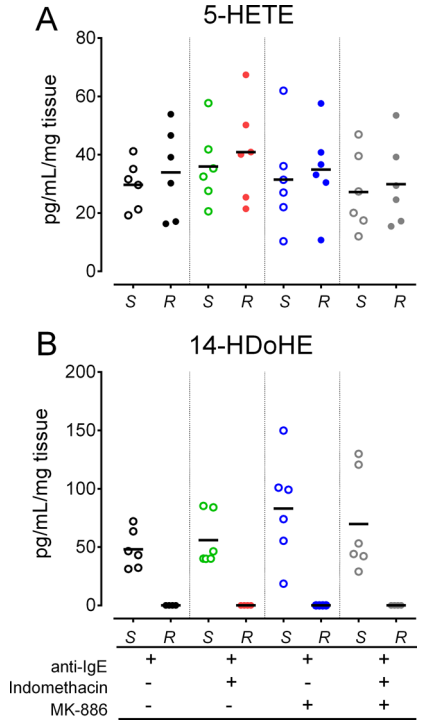

Figure 4. Stereochemistry of oxylipin production in human bronchus. The concentration of 5(*R*,*S*)-HETE (A) and 14(*R*,*S*)-HDoHE (B) in the organ bath demonstrate that 5-HETE is nonenzymatically produced, while 14-HDoHE is enzyme-derived following anti-IgE stimulation of the human bronchus. The tissue segments are from three patient donors in duplicates (total $n = 6$ per treatment). Hydroxyeicosatetraenoic acid (HETE), hydroxydocosahexaenoic acid (HDoHE).

raphy for determining the synthetic source of the released lipids. Analyses based upon standard chromatography risk making incorrect conclusions about the biochemical sources of the compounds.

Oxylipin Release Following 24-h Tissue Incubation. The oxylipin release profile was evaluated at an extended time point of 24 h by placing the stimulated human tissue in DMEM media overnight. In total, 25 oxylipins were detected, of which 14 were released from the stimulated human bronchus preparation and 11 were constituents of the DMEM incubation media. Interestingly, 4 of the oxylipins that were elevated with anti-IgE treatment originated from prostaglandin D_2 metabolism (PGD_2, 11β-$PGF_{2\alpha}$, PGJ_2, and $\Delta 12$-PGJ_2; $p < 0.05$; Figure 5A–D; Table S-9). The

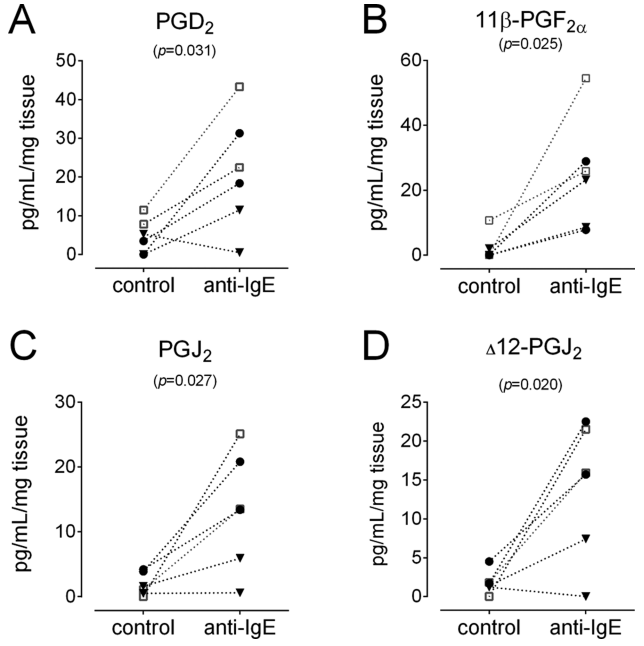

Figure 5. Oxylipin release after 24-h incubation of human bronchus. Following 60 min organ bath anti-IgE stimulation, human segments were incubated at 37 °C for 24 h in DMEM media. The observed levels of prostaglandin D_2 and its major metabolites were elevated compared to control treated tissue. Data represent replicated segments from three patient donors (patient 1(●), patient 2 (▼), patient 3 (□), $n = 6$). *P* values were determined using a paired *t* test. Phosphate buffer (PBS) serves as a negative control. Dulbecco modified eagle medium (DMEM).

significance of this prostaglandin release was strengthened by an almost complete loss (16% remaining) of PGD_2 following spiked media incubation under the same conditions but without tissue (Figure S-5). These findings suggest that the mast cells have a prolonged activation state.

Study Limitations. There are some method limitations that should be considered. The current SPE protocol was developed to extract a large number of analytes simultaneously and may therefore not be optimal for all species, as

Table 1. Enantiomeric Excess (ee) of Detectable Oxylipins for Each Treatment of Human Bronchus and Guinea Pig Trachea (Method C)[a]

	treatment	13(*S*)-HODE	9(*S*)-HODE	11(*S*)-HETE	12(*S*)-HETE	15(*S*)-HETE	5(*S*)-HETE	14(*S*)-HDoHE	17(*S*)-HDoHE
human	anti-IgE	23	33	0	100	6	−3	100	100
	anti-IgE, indomethacin	21	30	13	100	9	−5	100	100
	anti-IgE, MK-886	32	41	2	100	−28	−6	100	100
	anti-IgE, MK-886, indomethacin	22	31	6	100	14	−5	100	100
guinea pig	OVA	−10	15	−100[b]	100	ND	100	100	100
	OVA, indomethacin	−26	25	ND	100	ND	100	100	100
	OVA, MK-886	−10	16	−100[b]	100	ND	100	100	100

[a]For each treatment, enantiomeric excess (%) was determined by calculating the difference between average concentration for *S*- minus the *R*-enantiomer ($n = 6$), each expressed as % of total concentration ($R + S$), i.e., % conc. (S) − % conc. (R) = enantiomeric excess (%). FLAP/5-LOX inhibitor (MK-886), see Figure 1. Ovalbumin (OVA). Not detected (ND). [b]Signal is at limit of detection (LOD).

DOI: 10.1021/acs.analchem.8b01651
Anal. Chem. 2018, 90, 10239−10248

demonstrated by the relatively low recovery for some oxylipins. However, the extraction conditions can easily be altered if the analysis of specific oxylipins is required. Autoxidation may result in the rapid degradation of certain oxylipin species; however, this can be accounted for through the use of parallel tissue controls and chiral chromatography. The human bronchus preparation is derived from early stage cancer patients, of elderly age, which may bias the result compared to healthy and younger individuals. Human bronchus is also localized in the peripheral airways, while the guinea pig trachea is from the central airways. It is therefore likely that the cellular composition in the guinea pig trachea is different from that of the human bronchus and consequently release different oxylipins to a varying degree. Despite these shortcomings, the guinea pig is a useful model, closely resembling the human airway in terms of structure and function (as has been further demonstrated herein). The guinea pig therefore constitutes a translational model of interest for investigating further allergen induced airway responses, such as by pre-exposing intact tissue segments to the human allergen house dust mite or inflammatory cytokines.

CONCLUSIONS

Respiratory diseases such as asthma are characterized by variable airway obstruction and inflammation in both the large and small airways.[23] Current treatment strategies include targeting both bronchoconstriction and inflammation, in which signaling oxylipins can exert a modulating and mediating role. Investigating the oxylipin pathways involved in the inflammatory response and contracting airways is therefore of relevance to understanding disease mechanisms. We have demonstrated an interdisciplinary workflow that incorporates functional experiments of intact human and guinea pig airways with the simultaneous assessment of oxylipin biosynthesis. This shows how a pharmacological organ bath bioassay for functional experiments of intact human and guinea pig airways can be combined with LC−MS/MS for comprehensive oxylipin profiling. Our bioanalytical method, which includes an automated positive pressure SPE process, greatly facilitates sample processing and was able to detect a release of 57 oxylipins from human bronchus and 42 from guinea pig trachea. Pharmacological inhibition of COX and 5-LOX pathways resulted in changes in smooth muscle contractions, which after 60 min could be verified biochemically by shifts in the oxylipin levels from the corresponding molecular pathways. The synthetic route of 14- and 17-HDoHE production was shown to be due to 15-LOX activity, whereas observed 5-HETE was nonenzymatically produced (e.g., via lipid peroxidation). These findings provide increased insight into the activated biochemical pathways and it should be highlighted that the use of nonchiral chromatography could have led to incorrect conclusions on the synthetic origin of the monohydroxy fatty acids. Of possible relevance to bronchoconstriction in the airways, we observed that previously unexamined oxylipins were altered by the pharmacological interventions, including CYP450-derived EpOMEs and EpETrEs. These observations suggest future experiments to explore selective inhibitors or agonists/antagonists to identify causal mechanisms, as we previously reported for the role of PGE_2 in the human airways.[14] Finally, we report a sustained release of PGD_2 from human bronchus at 24 h after the last tissue stimulation in the organ bath. This is of particular interest as mast cells are important effector cells in asthma and other allergic diseases and suggest that they have a persistent activation status, maintained after the last anti-IgE stimulation. It should also be highlighted that this workflow can be applied in multiple research areas, including blood vessels, gastrointestinal segments, and urogenital organs. We propose that this combined workflow will aid in new therapeutic target assessment in the airways by linking relevant oxylipin biosynthetic routes to simultaneous smooth muscle contractions and signaling pathways in intact airway tissue.

ASSOCIATED CONTENT

Supporting Information

The Supporting Information is available free of charge on the ACS Publications website at DOI: 10.1021/acs.analchem.8b01651.

Detailed description of lipid nomenclature and Methods A−C (PDF)

AUTHOR INFORMATION

Corresponding Authors

*E-mail: craig.wheelock@ki.se. Phone: +46 8 524 87630.
*E-mail: sven-erik.dahlen@ki.se. Phone: +46 8 524 87203.

ORCID

Craig E. Wheelock: 0000-0002-8113-0653

Author Contributions

§J.K. and A.F. contributed equally to the manuscript. This work was planned and designed by all authors. J.K., A.F., J.S., and D.F. conceived of the experiments and performed the analysis. J.K., A.F., J.S., D.F., C.G., and C.E.W. interpreted the data and drafted the manuscript. M.A. and S.-E.D. critically reviewed the manuscript. All authors have given approval to the final version of the manuscript.

Notes

The authors declare no competing financial interest.

ACKNOWLEDGMENTS

A.F. was funded by the Karin and Sten Mörtstedt Initiative on Anaphylaxis. M.A., C.E.W., and S.-E.D. acknowledge the supportive grants received from the Swedish Heart-Lung Foundation (Grants 20170734, 20170603, 20150525, 20130636, 20150640, 20140469, 20140533), Swedish Research Council (Grants 2016-02798, 2014-3281), the Konsul Th C Berghs research foundation, the ChAMP (Centre for Allergy Research Highlights Asthma Markers of Phenotype) consortium, which is funded by the Swedish Foundation for Strategic Research, the Karolinska Institutet, AstraZeneca & Science for Life Laboratory Joint Research Collaboration, and the Vårdal Foundation.

REFERENCES

(1) Vane, J. *Nat.-New Biol.* **1971**, *231* (25), 232−235.
(2) Noonan, M. J.; Chervinsky, P.; Brandon, M.; Zhang, J.; Kundu, S.; McBurney, J.; Reiss, T. F. *Eur. Respir. J.* **1998**, *11* (6), 1232−1239.
(3) Dennis, E. A.; Norris, P. C. *Nat. Rev. Immunol.* **2015**, *15* (8), 511−523.
(4) Milne, G. L.; Yin, H.; Hardy, K. D.; Davies, S. S.; Roberts, L. J. *Chem. Rev.* **2011**, *111* (10), 5973−5996.
(5) Gerwick, W. H.; Moghaddam, M.; Hamberg, M. *Arch. Biochem. Biophys.* **1991**, *290* (2), 436−444.
(6) Dahlén, S. E.; Kumlin, M.; Granström, E.; Hedqvist, P. *Respiration* **2004**, *50* (Suppl2), 22−29.

DOI: 10.1021/acs.analchem.8b01651
Anal. Chem. 2018, 90, 10239−10248

(7) Singh, D.; Ravi, A.; Southworth, T. *Clin. Pharmacol.: Adv. Appl.* **2017**, *9*, 165−173.
(8) Simon, R. A.; Namazy, J. *Clin. Rev. Allergy Immunol.* **2003**, *24* (3), 239−251.
(9) Tahir, A.; Bileck, A.; Muqaku, B.; Niederstaetter, L.; Kreutz, D.; Mayer, R. L.; Wolrab, D.; Meier, S. M.; Slany, A.; Gerner, C. *Anal. Chem.* **2017**, *89* (3), 1945−1954.
(10) Colas, R. A.; Shinohara, M.; Dalli, J.; Chiang, N.; Serhan, C. N. *Am. J. Physiol. Cell Physiol.* **2014**, *307* (1), C39−54.
(11) Mazaleuskaya, L. L.; Salamatipour, A.; Sarantopoulou, D.; Weng, L.; FitzGerald, G. A.; Blair, I. A.; Mesaros, C. *J. Lipid Res.* **2018**, *59* (3), 564−575.
(12) von Euler, U. S. *J. Physiol.* **1936**, *88* (2), 213−234.
(13) Palmer, R. M.; Ferrige, A. G.; Moncada, S. *Nature* **1987**, *327* (6122), 524−526.
(14) Säfholm, J.; Manson, M. L.; Bood, J.; Delin, I.; Orre, A.-C.; Bergman, P.; Al-Ameri, M.; Dahlén, S.-E.; Adner, M. *J. Allergy Clin. Immunol.* **2015**, *136* (5), 1232−1239.e1.
(15) Säfholm, J.; Dahlén, S.-E.; Adner, M. *Eur. J. Pharmacol.* **2013**, *718* (1−3), 277−282.
(16) Rago, B.; Fu, C. *J. Chromatogr. B: Anal. Technol. Biomed. Life Sci.* **2013**, *936*, 25−32.
(17) Young, R. N. *Agents Actions Suppl.* **1991**, *34*, 179−187.
(18) Bäck, M. *Acta Physiol. Scand. Suppl.* **2002**, *648*, 1−55.
(19) Tabet, Y.; Sirois, M.; Sirois, C.; Rizcallah, E.; Rousseau, É. *Am. J. Physiol. Lung Cell. Mol. Physiol.* **2013**, *304* (8), L562−569.
(20) Smith, K. R.; Pinkerton, K. E.; Watanabe, T.; Pedersen, T. L.; Ma, S. J.; Hammock, B. D. *Proc. Natl. Acad. Sci. U. S. A.* **2005**, *102* (6), 2186−2191.
(21) Balgoma, D.; Yang, M.; Sjödin, M.; Snowden, S.; Karimi, R.; Levänen, B.; Merikallio, H.; Kaarteenaho, R.; Palmberg, L.; Larsson, K.; et al. *Eur. Respir. J.* **2016**, *47* (6), 1645−1656.
(22) Dumlao, D. S.; Cunningham, A. M.; Wax, L. E.; Norris, P. C.; Hanks, J. H.; Halpin, R.; Lett, K. M.; Blaho, V. A.; Mitchell, W. J.; Fritsche, K. L.; et al. *J. Nutr.* **2012**, *142* (8), 1582−1589.
(23) Papi, A.; Brightling, C.; Pedersen, S. E.; Reddel, H. K. *Lancet* **2018**, *391* (10122), 783−800.
(24) Schneider, C.; Brash, A. R. *Prostaglandins Other Lipid Mediators* **2002**, *68*−*69*, 291−301.

DOI: 10.1021/acs.analchem.8b01651
Anal. Chem. 2018, 90, 10239−10248